Nuclear Engineering and Technology 50 (2018) 1190–1197

Contents lists available at ScienceDirect

Nuclear Engineering and Technology

journal homepage: www.elsevier.com/locate/net

Technical Note

Modeling of central void formation in LWR fuel pellets due to high-temperature restructuring

Grigori Khvostov

Paul Scherrer Institut, CH 5232, Villigen, PSI, Switzerland

ARTICLE INFO

Article history:
Received 9 June 2018
Received in revised form
4 July 2018
Accepted 9 July 2018
Available online 12 July 2018

Keywords:
GRSW-A model
FALCON code
High-temperature restructuring
Central void formation

ABSTRACT

Analysis of the GRSW-A model coupled into the FALCON code is extended by simulation of central void formation in fuel pellets due to high-temperature fuel restructuring. The extended calculation is verified against published, well-known experimental data. Good agreement with the data for a central void diameter in pellets of the rod irradiated in an Experimental Breeder Reactor is shown. The new calculation methodology is employed in comparative analysis of modern BWR fuel behavior under assumed high-power operation. The initial fuel porosity is shown to have a major effect on the predicted central void diameter during the operation in question. Discernible effects of a central void on peak fuel temperature and Pellet-Cladding Mechanical Interaction (PCMI) during a simulated power ramp are shown. A mitigating effect on PCMI is largely attributed to the additional free volume in the pellets into which the fuel can creep due to internal compressive stresses during a power ramp.

1. Introduction

It has been known since long [1] that a high-temperature irradiation of the uranium-dioxide, or MOX fuels results in local restructuring of the fuel in the central pellet zone, where certain temperature is exceeded, viz.: 1350–1400 °C for equiaxed-grain growth, and 1600–1700 °C for columnar grain structure formation. These processes are accompanied by sweeping-out of as-fabricated pores and increase in local fuel density, which eventually results in a formation of the void in the centre of the pellet.

Extensive fuel restructuring zones with a formation of sizable central voids was widely observed in fuel rods after irradiation in Fast Breeder Reactors (FBR) [2]. On the other hand, occurrence of high-temperature restructuring, resulting in considerable effects on fuel rod behavior, is less likely during commercial irradiation in Light-Water Reactors (LWR), because of relatively low linear-heat-generation rate (LHGR) at normal operation. Consequently, these effects are often neglected by computational codes involved in the analysis of LWR fuel reliability and safety. For example, corresponding simulation was, till recently, out of the scope of an advanced version of the FALCON code [3], which has been developed and extensively employed at Paul Scherrer Institut (PSI) in Switzerland [4].

It is to be noted, however, that the normal operation of fuel rods in LWRs has been usually carried out with significant margins of the peak LHGR to a maximum permitted power, conventionally referred to as Thermo-Mechanical Operational Limit (TMOL). Typical examples of a real operation history and TMOL for modern BWR fuel are presented in Fig. 1, showing a difference by nearly a factor of ~2 in this specific case. A TMOL for a specific fuel design and operational conditions is normally deduced by fuel vendors, in the form of a LHGR limit in function of local pellet-averaged burnup, based on conservative calculation with validated fuel behavior codes [5]. The Nuclear Power Plant (NPP) has been ensured that the lasting, continuous operation with the power history in question cannot result in a rod failure by any of known, proven mechanisms. Some of these calculations show that, for irradiation with TMOL, high-temperature fuel re-structuring and its consequences are to be expected, as it can be seen from Fig. 2.

Apart from the hypothesized TMOL power histories, intensive power ramps in LWR fuel rods were shown to be able to eventually result in a discernible high temperature restructuring and central void formation (see e.g. Fig. 9 in Ref. [6]). A missing model for the appropriate effect was mentioned in the discussion of Ref. [7] as a likely reason of some code over-prediction for Fission Gas Release (FGR) in a specific case of a ramp-tested rodlet with a high Ramp Terminal Level (RTL) and long high-power conditioning. Indeed, it has been known that the presence of a central void reduces fuel temperature [1] – basically, due displacement of the heat

E-mail address: grigori.khvostov@psi.ch.

https://doi.org/10.1016/j.net.2018.07.003

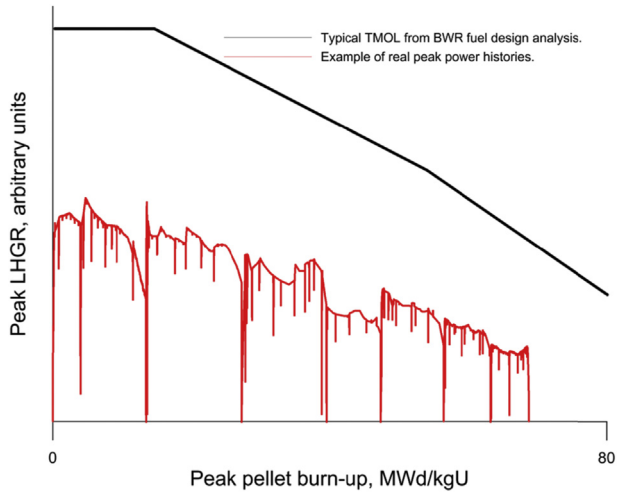

Fig. 1. Comparative examples of TMOL and real power histories for modern BWR fuels.

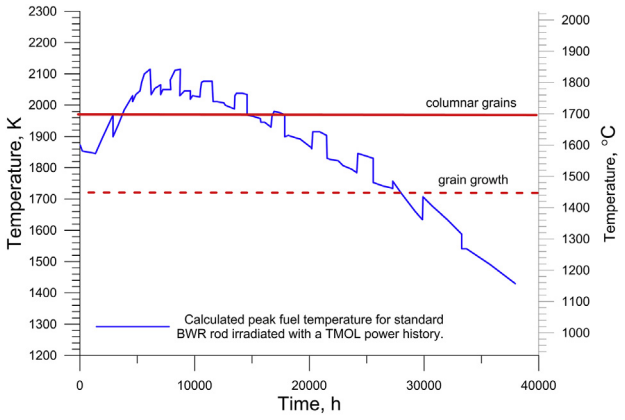

Fig. 2. Calculated peak central-line fuel temperature during irradiation with TMOL power history.

generation outward, closer to the heat-exchanging surface (i.e. the pellet-cladding interface). Besides, analysis of power ramps in fuel rods with initial, as-fabricated central voids [8] showed a discernible mitigation of the Pellet-Cladding Mechanical Interaction (PCMI), in comparison to a solid-pellet rod. The effect was related to the as-fabricated central hole in the pellets that turned out to be fully filled up after the power ramp, due to fuel creep during the PCMI.

Last but not least, the phenomenon in question may eventually become relevant to the current concepts of Accident Tolerant Fuel (ATF) [9]. For example, one of the important issues related to the use of SiC-based claddings is the low thermal conductivity, in comparison to the standard zircaloys. The direct consequence will be an increase in fuel temperature [10]. This may enhance the processes of fuel restructuring and, eventually, lead to a central void formation in the pellets during the base irradiation. On the other hand, the increased compliance of a pellet with a central void could, to some degree, counteract the low resistance of SiC-based cladding to PCMI failure due to its brittle property.

Obviously, the code analysis as applied to aforementioned cases would be more adequate and, most likely, less conservative given the effects in question are taken into consideration. Specifically, the presence of a central void and the increase in local density will result in a decrease in peak fuel temperature and mitigation of the PCMI.

The capability of the GRSW-A models integrated into the FALCON code has been recently extended by simulation of central void formation and growth in fuel pellets under high-temperature irradiation. The current model addressed the effect of high-temperature restructuring on the initial, as-fabricated porosity. The pellet void volume is correlated with the degree of equiaxed-grain growth, which has been simulated in the original GRSW-A model [11]. The model in question is described in Chapter 2.

The model coupling to the integral fuel rod behavior calculation of the FALCON and GRSW-A codes is described in Chapter 3. The results of application of the extended codes to the two fuel types are presented and discussed in Chapter 4.

2. The model

The GRSW-A model, integrated into the FALCON fuel behavior code [12], has incorporated a model for high-temperature fuel restructuring. Specifically, the equiaxed-grain growth was simulated in GRSW-A as isotropic aggregation of the grains, using the modified equation from Ref. [13]:

$$\frac{dR_g}{dt} = k_0 exp\left(-\frac{E_{g.growth}}{kT}\right)\left(\frac{1}{R_g}-\frac{1}{R_{g.max}}\right) \times \left(1-\left(\frac{S_F}{V}\right)_{open}\left(\frac{S_F}{V}\right)_{tot}^{-1}\right) \quad (1)$$

$$R_{g.max} = k_1 exp\left(-\frac{k_2}{T}\right) \quad (2)$$

where k_0,k_1,k_2, are constant coefficients, $E_{g.growth}$ the activation energy, $R_{g.max}$ the limiting grain radius for the current temperature, k Boltzmann constant, $(S_F/V)_{open}$ and $(S_F/V)_{tot}$ the open- and total-specific areas of the grain boundaries.

Reduction of specific number densities of modelled microstructural objects, associated with grain boundaries (such as the emergent gaseous pores and gas-atom clusters), due to the equiaxed-grain growth was related to the calculated increase in the relative fuel volume, f_{rstr}, affected by the fuel restructuring in question:

$$f_{rstr} = \frac{\Delta V_g}{V_g} \quad (3)$$

where ΔV_g is the increase in the grain volume due to the high-temperature equiaxed-grain growth, V_g the current volume of the grain.

Similarly, the current model correlates the relative volumetric change of the affected pellet zones due to grain growth-stipulated reduction of the initial fuel porosity caused by dimensionally stable, large, inter-granular pores, P_{as-f}, with the restructured fuel fraction, which is expressed by Eq. (4):

$$\frac{\Delta V}{V_0} = -P_{as-f} \times f_{rstr} \quad (4)$$

The cross-section area of the emergent central void, A_{void}, is calculated by numerical integration of the decreases in cross-section areas of the coaxial layers in the radial pellet mesh, dA, over the pellet radius:

$$A_{void} = \int_0^{R_{pellet}} dA \quad (5)$$

where dA is calculated from:

$$\frac{dA}{A_0} = k_a \frac{dV}{V_0} \tag{6}$$

The coefficient k_a in Eq. (6) accounts for anisotropy in the dimensional changes of the axisymmetric fuel layers due to divergence of the as-fabricated pores. The coefficient can take values in the range from 2/3 to unity, which corresponds to fully-isotropic (i.e. the relative volumetric and linear deformations are related as $\varepsilon_v/3 = \varepsilon_{ii}$) and anisotropic (i.e. the volumetric change is equal to the change of the cross-section area) case, respectively. The anisotropy is expected to arise from the effect of high temperature gradients in fuel pellets [14]. In other words, the current model assumes an anisotropic grain-growth and increase in fuel density to be related to the radial migration of the relatively large, as-fabricated grain-boundary pores up the temperature gradient in the pellet, which results in formation of a central void, as schematically shown in Fig. 3.

Finally, for the discrete radial pellet-mesh, the radius of central void during a simulated high-temperature restructuring, is calculated as function of time:

$$R_{void} = \sqrt{A_{void}/\pi} = R_{pellet}\left[k_a P_{as-f} \sum_{i=1}^{N-zones} \varepsilon_i f_{rstr\ (i)}\right]^{1/2} \tag{7}$$

where R_{void} is the void radius, R_{pellet} the pellet radius, $P_{as\text{-}f}$ the as-fabricated porosity, ε_i the relative volume of the i-th node in the radial pellet mesh, $f_{rstr\ (i)}$ the local fraction of restructured fuel, k_a the anisotropy coefficient.

3. Implementation of the model with an advanced version of the FALCON code

The FALCON code [3] does not allow for an automated transition from a solid-to annular-pellet geometry within a single-run simulation period. Besides, while the strain-displacement relations for the cladding are based on the large deformation theory, the small deformations are assumed for the fuel. On the other hand, node displacements in the central area of the pellet mesh affected by high-temperature restructuring and central void formation can be significant. This made it difficult to implement a close coupling of the above described model into the integral analysis of the FALCON code with the GRSW-A model.

To circumvent this issue, a FALCON based methodology was developed using a special procedure of the recursive restart of calculation. The methodology implies basically a periodic update of the pellet mesh, as shown in Fig. 4, over the multiple restarts. The nomenclature used in Fig. 4 is described in Table 1. In the beginning of each time-integration step, the code restart is carried out [15]. The central void diameter as function of an axial position is updated by modifying radial coordinates of the nodes in the inner part of the fuel mesh, which are introduced through the MODEL command card of the FALCON input file [16]. The updated coordinates for the pellet inner nodes at the end of the previous time-integration step are calculated with Eq. (7) after reading and processing of the results of the GRSW-A model, integrated into FALCON.

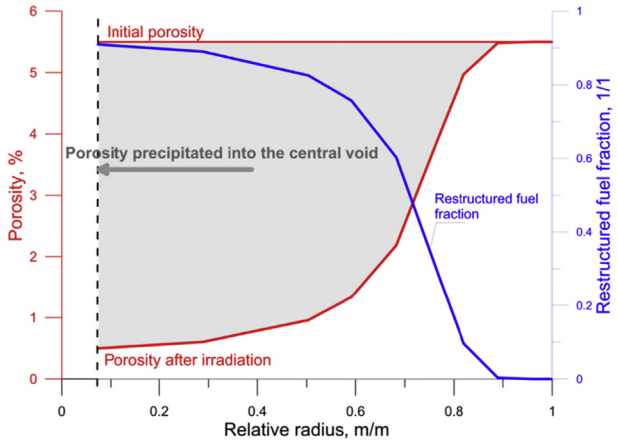

Fig. 3. Estimated radial profiles of local fraction of the restructured fuel and as-fabricated porosity after irradiation with a reference TMOL power history.

4. Results and discussion

4.1. Verification against the data for specific low-density MOX fuel irradiated in FBR

On the first step, the above described methodology was verified against the well-known experimental data [2]. A fuel rod with the low-density (83 %TD) MOX (UO_2 - 20% wt. PuO_2) fuel was irradiated in an FBR under high-power conditions (a peak local LHGR of 56 kW/m), which resulted in formation of a sizable central void in fuel pellets. The main parameters of rod design and irradiation conditions, assumed in the calculation are presented in Table 2.

Post Irradiation Examination of the rod in question showed extensive fuel restructuring, noting that no indications of fuel melting were found. While the pellets initially had no central void, the one with a diameter of 1.9 mm was observed by the destructive PIE (see Fig. 1 in Ref. [2]).

The calculation of the case in question was performed with the FALCON code coupled with the GRSW-A model, using the new methodology for evaluation of the effects of central void formation, as described in Chapter 3. The built-in models of the FALCON code for MOX fuel were employed [16], viz.: radial power distribution, fuel thermal conductivity, fuel melting temperature, mechanical and thermal properties of the stainless steel cladding SS304. An appropriate value for a theoretical density of the MOX fuel was input in the GRSW-A model. Apart from this, the UO_2 specific parameters were used in the GRSW-A calculation.

As shown in Fig. 5, the predicted centre-line fuel temperature in the peak-power node of the fuel rod is very high, approaching the melting point immediately after the first power increase to the maximum value of 56 kW/m. However, a drastic drop-down of the temperature, by ~400 K, due to the simulated formation of a central void is predicted. To all appearance, the decrease in temperature prevented a local fuel melting, in agreement with the experimental data [1].

As seen in Fig. 6, a large central void is predicted to emerge just in a few hours after the beginning of the irradiation considered. Note that different initial time integration steppings were tested with a view to verifying the convergence of the calculation results under the relatively fast processes as predicted in the beginning of this high-power irradiation. The smooth functions were thus obtained for the main figures of merit, such as central-void diameter and peak centre-line temperature. As also shown in Fig. 6, the solutions for different initial time-steps used by the explicit schema, as described in Chapter 3, shows up a discernible difference only during the first hour of the assumed irradiation. However, regardless the initial time-stepping, the solutions totally converge after ~5 h into this specific high-power irradiation.

The increase in central void diameter is predicted to be entirely saturated after ca. 500 h of irradiation with a maximum power of 56 kW/m. The calculated diameter of a central void in the Peak Power Node (PPN) at End-of-Life (EOL) amounts to 2.1 mm, which

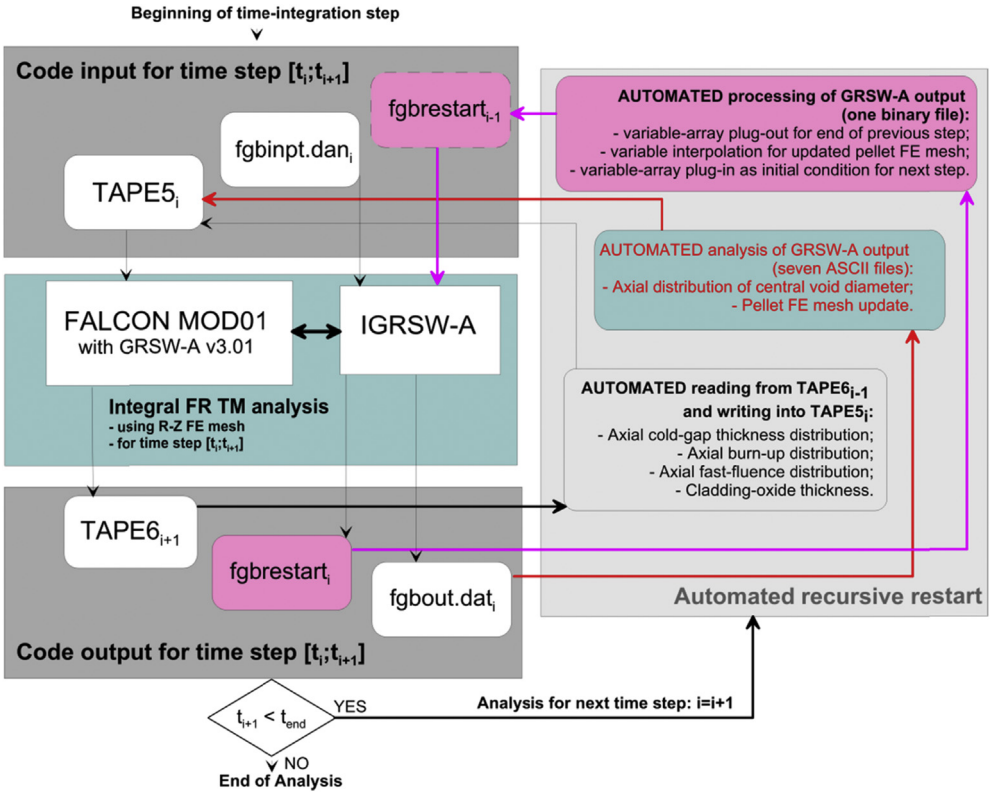

Fig. 4. Calculation flow-chart for simulation of integral effects of fuel restructuring with the advanced FALCON code.

Table 1
Nomenclature used in flow-chart of Fig. 4.

TAPE5	ASCII file containing all input for standard FALCON MOD01
fgbinp.dan	ASCII file containing supplementary input for Integrated GRSW-A analysis, e.g.: parameters of numerical methods, restart mode, GRSW-A model parameters, etc.
fgbrestart	Binary file containing the whole array of time-dependent GRSW-A variables for all integration points of pellet mesh and all time steps.
TAPE6	ASCII file containing all output results of standard FALCON MOD01.
fgbout1.dat	Seven ASCII files containing extended output results of Integrated GRSW-A for all integration points of pellet mesh and selected time steps, e.g.: spatial distribution of retained gas, grain-size distribution, porosity fractions, etc.
…	
fgbout7.dat	
FE	Finite Element
FR	Fuel Rod
IGRSW-A	Version of GRSW-A integrated into FALCON MOD01

Table 2
Parameters of fuel rod design and irradiation conditions according to the data [2] used for model verification.

Parameter, units	Value
Pellet geometry	Solid
Pellet material	$UO_2 - 20$ % wt. PuO_2
Assumed fuel grain size, μm	10
Pellet outer diameter, mm	6.45
Fuel density, %TD	83
Active fuel stack length, mm	292
Cladding material	Stainless Steel SS304
Cladding inner diameter, mm	6.987
Cladding outer diameter, mm	7.520
Place of irradiation	Experimental Breeder Reactor (EBR)
Maximum LHGR, kW/m	56
Assumed axial power profile shape	Truncated cosine
Assumed form factor of axial power distribution, 1/1	1.4
Coolant conditions	Sodium at 773 K and 5 bar
Cladding outer surface temperature, K	843
Peak fuel burnup at EOL, % FIMA	2.7

compares well with the measurement (Fig. 7). The good agreement was obtained noting that the highest anisotropy in the porosity divergence ($k_a = 1$ in Eq. (7)) was assumed. This value has been currently accepted for further applications.

According to the measurement and calculation, a diameter of the central void was very significant, amounting to ca. 30% of the initial pellet diameter. The volume of the central void equaled ca. 9% of the total pellet volume. This suggests that slightly more than 50% of the initial, very high porosity (ca. 17 vol%, according to the low initial density, as specified in Table 2) was transported to the pellet centre during the specific irradiation considered.

4.2. Application to modern BWR fuel under high-power irradiation

On the next step, the new methodology was applied to a modern BWR rod of 10 × 10 Fuel Assembly Design, assuming hypothesized irradiation with the TMOL power history, as schematically shown in Fig. 1. The parameters of fuel rod design are omitted here, as it was described in detail in the previous publications [17].

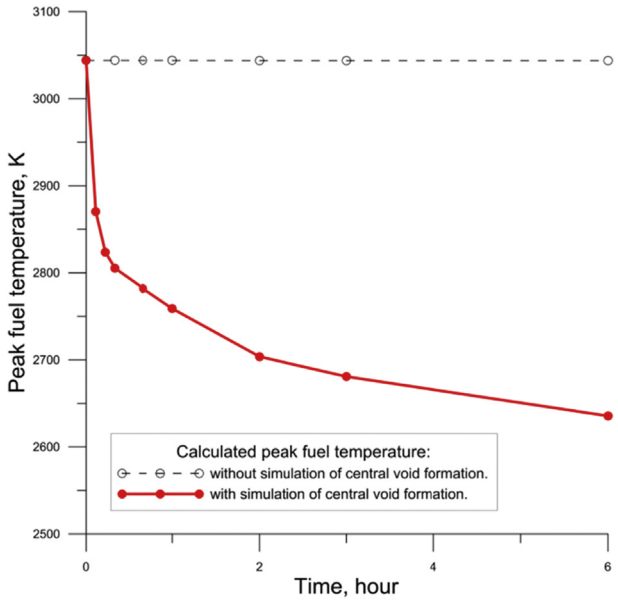

Fig. 5. Calculated centre-line fuel temperature in the beginning of the modelled irradiation [2].

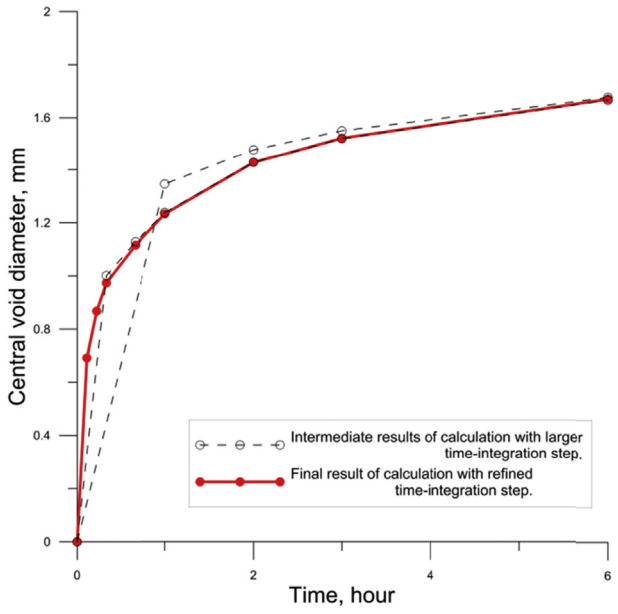

Fig. 6. Calculated central void diameter in the beginning of the modelled irradiation [2].

Essentially, the current calculation focused on a comparative analysis of the fuels with different parameters of the initial fuel structure, specifically grain size and fuel density (i.e. initial as-fabricated porosity), hereinafter referred to as 'Standard' and 'Advanced' fuel, as specified in Table 3.

The predicted central void diameter at EOL and the effect on peak fuel temperature during operation turned out to be more significant in the standard fuel, than in the advanced one, as shown in Fig. 8 and Fig. 9(a and b), respectively. As it can be seen from Fig. 9(b), the central void formation in the standard fuel resulted in a reduction of maximum fuel temperature to virtually the same level as in the advanced fuel. The larger central void, predicted for the standard fuel, is largely due to a higher initial porosity, to be

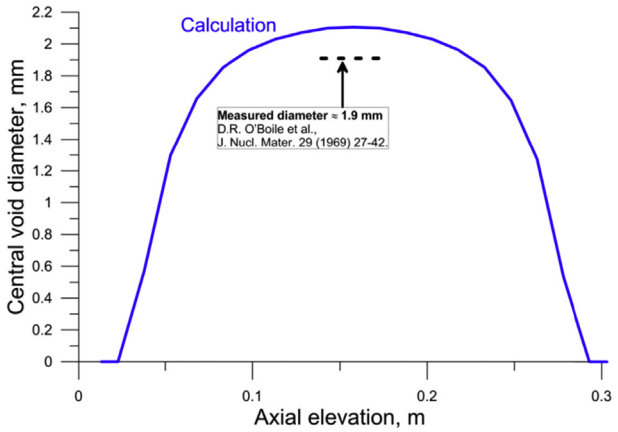

Fig. 7. Calculated axial profile of central void diameter after the modelled irradiation against experimental data [2].

Table 3
Parameters of the two BWR fuel types addressed by the comparative analysis.

Fuel type designation	Standard	Advanced
Fuel density, % TD	94.5	97.5
Grain size, μm	7.0	25.0
Initial pellet geometry	Solid	
Fuel material	UO_2 enriched with 5 % wt. U^{235}	
Cladding material	Zry-2	
FA design	BWR 10 × 10	

converted into the central void. Note that the three small maxima in the axial profiles, as shown in Fig. 8, are due to simulated periodic shift of the PPN position (from the top-, to middle-, and to bottom of the active stack), which is also depicted by 'fluctuations' of the temperature in Fig. 9(a). Nearly negligible effects were obtained for the advanced fuel, due to a very small, ca. 0.2 mm void, as shown in Fig. 8.

Consequently, considerable effect of central void formation on fission gas release (FGR) and internal gas pressure for the standard rod was predicted, as shown in Figs. 10 and 11, respectively. The effect on FGR is largely due to lower fuel temperature. The decrease in rod internal pressure is predicted due to a combination of the lower FGR and larger free volume in a rod with central voids in pellets. In fact, as the two values just mentioned are deemed to be critical for the rod reliability, including the phenomenon in question into the corresponding fuel design analysis seems to be necessary, noting e.g. a direct implication of the internal gas pressure in prediction of the so-called cladding 'lift-off' [18].

Furthermore, an analysis was carried out for the effects of central voids on thermal-mechanical behavior of the standard rod. To this end, a relatively fast power ramp was simulated at the end of base irradiation with the TMOL power history (i.e., at a peak pellet burnup of 78 MWd/kgU), assuming linearly increasing LHGR from the steady-state level to a specified Ramp Terminal Level (RTL = 350% TMOL), during 60 s. The calculated peak hoop-stress and strain in cladding of the standard rod are shown in Figs. 12 and 13, respectively.

As seen in Fig. 12, accounting for the presence of a central void resulted in a considerable decrease in the predicted hoop stress during the power ramp, as well as a delayed transition to the plastic deformation mode (the plateau on a stress-vs-power diagram) – approximately, by a factor of 1.3, in terms of power ramp level. Also, an increasing margin to the 1% total strain limit [19], resulting from the presence of a central void, can be seen in Fig. 13.

Quite explicably, the results of calculation, presented in Fig. 14,

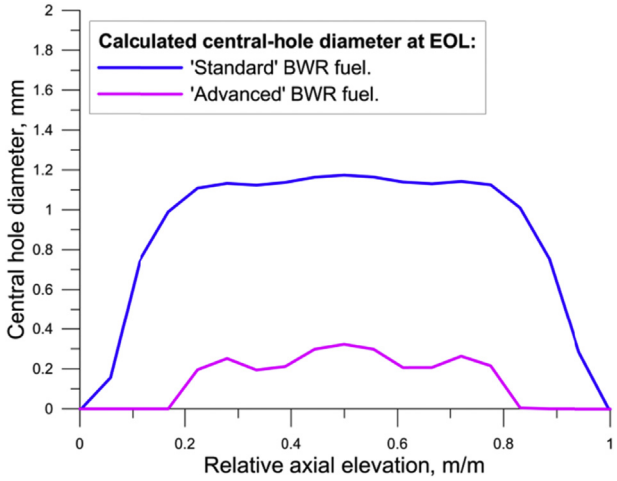

Fig. 8. Predicted axial profile of central void diameter after assumed irradiation with TMOL power history.

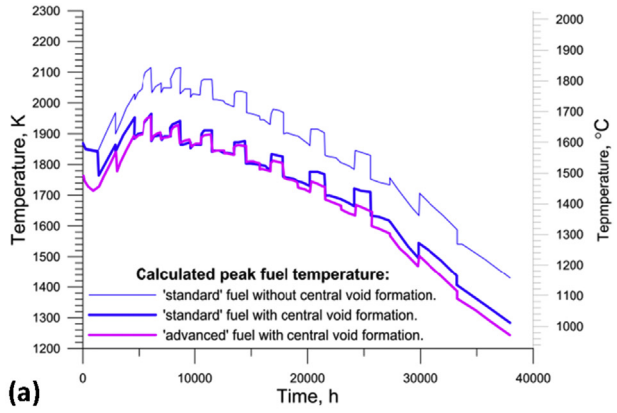

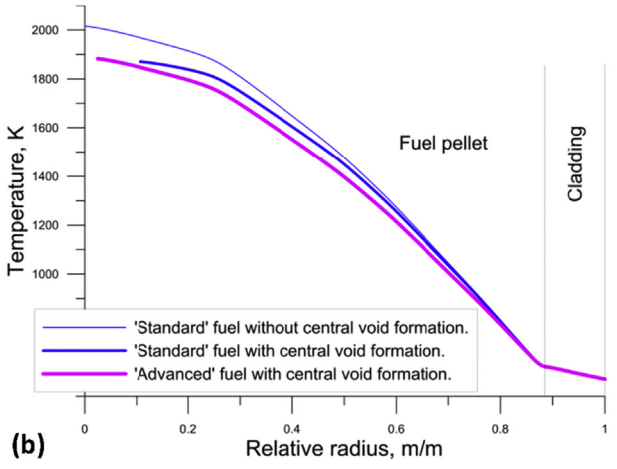

Fig. 9. (**a**) Predicted peak fuel temperature during assumed irradiation with TMOL power history. (**b**) Predicted temperature distributions across the rod radius at a time t = 5354 h of the simulated irradiation history.

show a decrease in fuel temperature during the power ramp, which suggests an increasing margin to the melting point. However, the temperature variation in the pellet with the central void, over the power ramp, does not decrease in comparison to the solid pellet. Therefore, an assumption can be made on that the predicted mitigating effect on PCMI is basically due to fuel creep into the

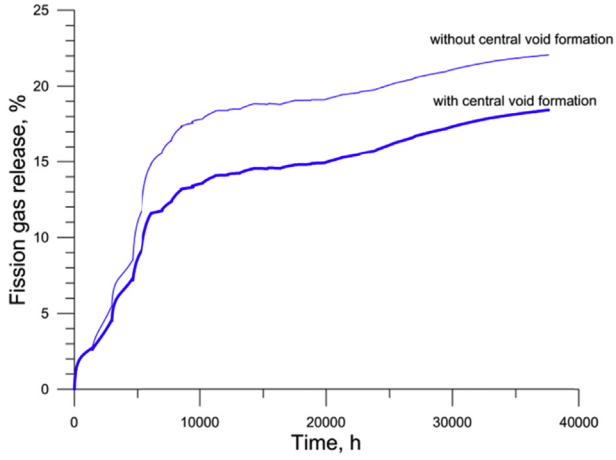

Fig. 10. Predicted FGR during assumed irradiation with TMOL power history.

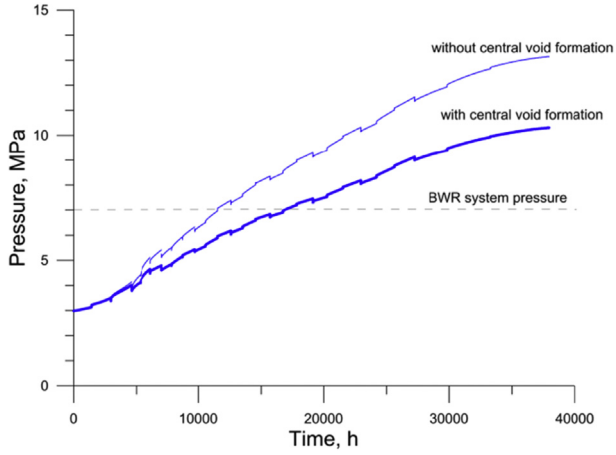

Fig. 11. Predicted rod internal pressure during assumed irradiation with TMOL power history.

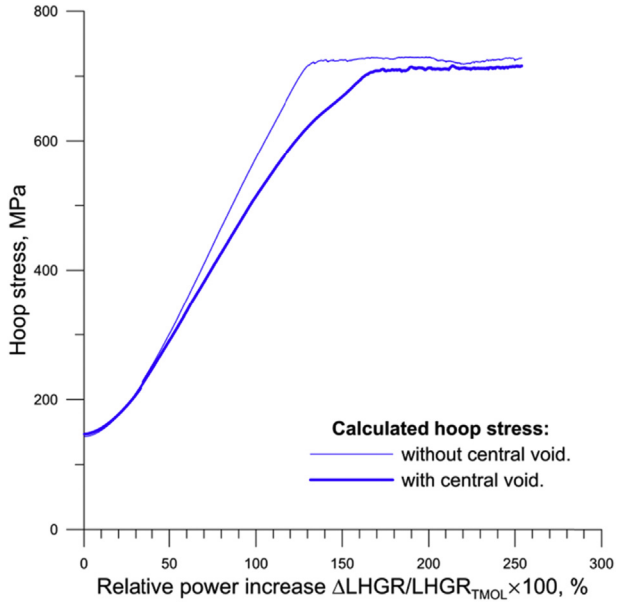

Fig. 12. Predicted peak hoop stress in cladding of the standard rod during simulated power ramp.

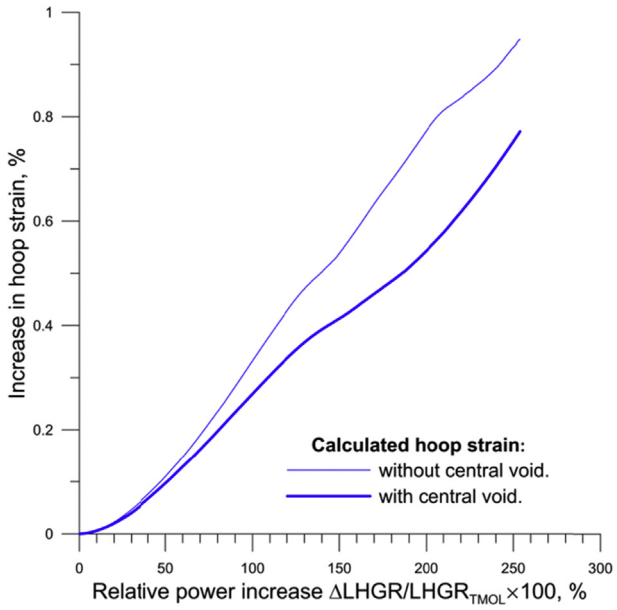

Fig. 13. Predicted peak hoop strain in cladding of the standard rod during simulated power ramp.

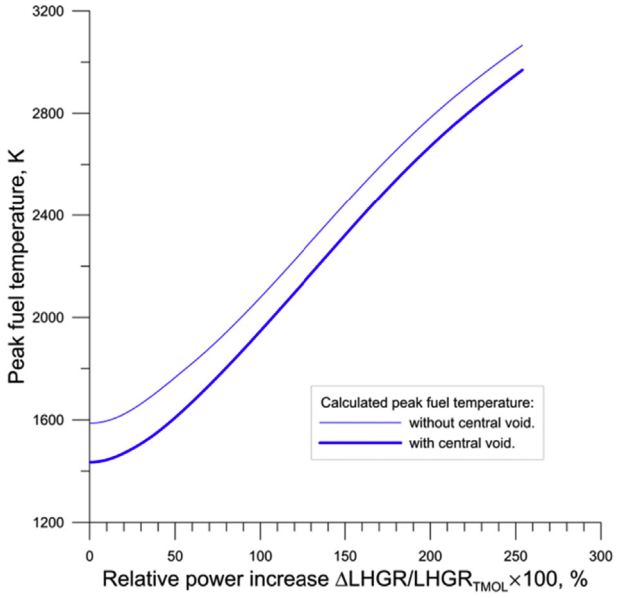

Fig. 14. Predicted peak fuel temperature in the standard rod during simulated power ramp.

central void. To verify this inference, an additional calculation was performed assuming radial displacement-constraint boundary conditions, imposed on the inner nodes of the annular pellet (see inserted drawing of a fragment of the fuel rod mesh in Fig. 15). As shown in Fig. 15, when inhibiting the fuel creep deformation into the void volume, the mitigating effect of the central void on PCMI (e.g., cladding hoop strain) is virtually vanished.

5. Conclusions

A simple model for the central void formation in fuel pellets during steady-state high-power irradiation was proposed. A special methodology was developed for model coupling into the integral

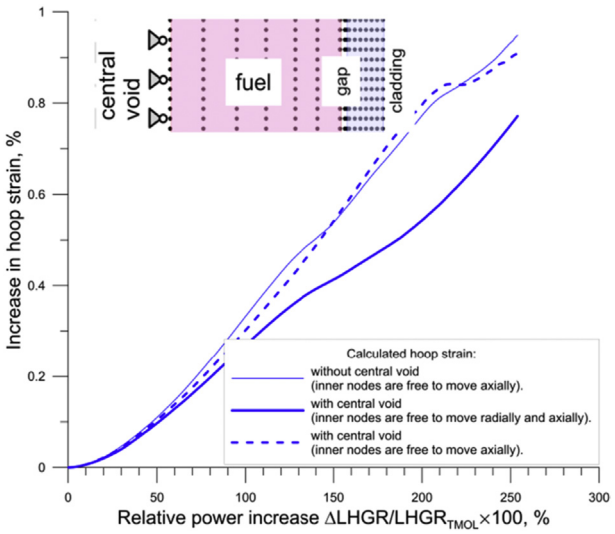

Fig. 15. Predicted peak hoop strain in cladding of the standard rod during simulated power ramp using different assumptions on the fuel creep into the void volume.

analysis of the FALCON code with the GRSW-A model for fission gas release and swelling in the fuel.

The extended calculation was verified against the published, well-known experimental data for a high-temperature irradiated, low-density MOX fuel. Good agreement with the results of Post-Irradiation Examination for a central void diameter in pellets of the rod was shown.

The new calculation methodology was employed in comparative analysis of modern BWR fuel behavior under assumed high-power operation. Discernible effect of a central void formation on peak fuel temperature, and Pellet-Cladding Mechanical Interaction (PCMI) during a simulated power ramp was shown. The initial fuel porosity was shown to have a major effect on the predicted central void diameter during the operation in question. A mitigating effect on PCMI was largely attributed to the additional free volume in the pellets into which the fuel can creep due to internal compressive stresses during a power ramp.

The new model and FALCON based methodology can be employed in the future for the reduction of the conservatisms within the standard fuel design analysis, dealing with hypothesized high-power histories of operation. Another potential field of application may be analysis of different Accident Tolerant Fuel (ATF) concepts, particularly those employing high-compliance ('soft') pellet types for mitigating the PCMI.

Declarations of interest

None.

Acknowledgement

The presented model and methodology were developed at Paul Scherrer Institute in the framework of the STARS program, as part of technical service performed for the Swiss Federal Nuclear Safety Inspectorate (ENSI). The study was reported by the author as a keynote presentation to the OECD Nuclear Energy Agency Workshop on Nuclear-Fuel Modelling to Support Safety and Performance Enhancement for Water-Cooled Reactors, Paris, France, 7–9 March 2017.

Dr. Cozzo, Cedric (Paul Scherrer Institut, Switzerland) is acknowledged with thanks for his review of the paper manuscript.

References

[1] D.R. Olander, Fundamental Aspects of Nuclear Reactor Fuel Elements, TID-26711-P1, National Technical Information Services, 1976, pp. 113–144.

[2] D.R. O'Boyle, F.L. Brown, J.E. Sanecki, Solid fission product behavior in Uranium-Plutonium oxide fuel irradiated in a fast neutron flux, J. Nucl. Mater. (1969) 27–42.

[3] Y.R. Rashid, R.S. Dunham, R.O. Montgomery, FALCON MOD01: Fuel Analysis and Licensing Code – Volume 1: Theoretical and Numerical Bases, EPRI Report 1011307, December 2004.

[4] G. Khvostov, A dynamic model for fission gas release and gaseous swelling integrated into the FALCON fuel analysis and licensing code, in: Proc.: TOP Fuel 2009, Paris, France, September 6-10, 2009.

[5] A. Medvedev, S. Bogatyr, V. Kouznetsov, G. Khvostov, V. Lagovsky, L. Korystin, V. Poudov, Fuel rod behavior at high burnup WWER fuel cycles, in: Proc.: 5th International Conference on WWER Fuel Performance, Modeling and Experimental Support. 29 September – 3 October, Congress Center Albena, Bulgaria, 2003.

[6] V.I. Arimescu, I. Vallejo, J. Karlsson, G. Zhou, G. Grandi, P. Raynaud, Y. Yun, N. Doncel, J. Sercombe, M. Pytel, M. Dostal, R. Dunavant, J.S. Yoo, Third SCIP modeling Workshop: beneficial impact of slow power ramp on PCI performance, in: Proc.: Water Reactor Fuel Performance Meeting WRFPM 2014, Sendai, Japan, Sep. 14-17, 2014.

[7] L.E. Herranz, I. Vallejo, G. Khvostov, J. Sercombe, G. Zhou, Assessment of fuel rod performance codes under ramp scenarios investigated within the SCIP project, Nucl. Eng. Des. 241 (2011) 815–825.

[8] V. Novikov, A. Medvedev, G. Khvostov, S. Bogatyr, V. Kuznetsov, L. Korystin, Modelling of thermal mechanical behaviour of high burn-up VVER fuel at power transients with especial emphasis on impact of fission gas induced swelling of fuel pellets, in: Proc.: OECD Seminar on Pellet-clad Interaction in Light Water Reactor Fuels, AIX EN PROVENCE, France, March 9-11, 2004.

[9] Zhengang Duan, Huilong Yang, Yuhki Satoh, Kenta Murakami, Sho Kano, Zishou Zhao, Jingjie Shen, Hiroaki Abe, Current status of materials development of nuclear fuel cladding tubes for light water reactors, Nucl. Eng. Des. 316 (2017) 131–150.

[10] C. Cozzo, S. Rahman, SiC cladding thermal conductivity requirements for normal operation and LOCA conditions, PNE (Protein Nucleic Acid Enzyme) 106 (2018) 278–283.

[11] G. Khvostov, A. Medvedev, S. Bogatyr, The dynamic model of grain boundary processes in high burn-up LWR fuel and its application in analysis by the START-3 code, in: Proc.: International Conference on WWER Fuel Performance, Modeling and Experimental Support, Albena-Varna, Bulgaria, September 29-October 3, 2003.

[12] G. Khvostov, K. Mikityuk, M.A. Zimmermann, A model for fission gas release and gaseous swelling of the uranium dioxide fuel coupled with the FALCON code, Nucl. Eng. Des. 241 (2011) 2983–3007.

[13] J.B. Ainscough, B.W. Oldfield, J.O. Ware, Isothermal grain growth kinetics in sintered UO_2 pellets, J. Nucl. Mater. 49 (1974) 117–128.

[14] Michael R. Tonks, Yongfeng Zhang, Xianming Bai, Paul C. Millett, Demonstrating the Temperature Gradient Impact on Grain Growth in UO_2 Using the Phase Field Method, Materials Research Letters (2013), https://doi.org/10.1080/21663831.2013.849300.

[15] F. Ribeiro, G. Khvostov, Multi-scale approach to advanced fuel modelling for enhanced safety, Prog. Nucl. Energy 84 (2015) 24–35.

[16] Fuel Analysis and Licensing Code: FALCON MOD01: Volume 2: User's Manual, EPRI, Palo Alto, CA, 2004, p. 1011308.

[17] G. Ledergerber, S. Valizadeh, J. Wright, M. Limbäck, L. Hallstadius, D. Gavillet, S. Abolhassani, F. Nagase, T. Sugiyama, W. Wiesenack, T. Tverberg, Fuel behaviour beyond design - exploring the limits, in: Proc.: Water Reactor Fuel Performance Meeting, WRFPM 2008, Seoul, Korea, 19–23 October, 2008.

[18] G. Khvostov, W. Wiesenack, Analysis of selected Halden overpressure tests using the FALCON code Nuclear Engineering and Design, Nucl. Eng. Des. 310 (2016) 395–409.

[19] (USNRC SRP 4.2), NUREG-0800 Rev. 3, US Nuclear Regulatory Commission Standard Review Plan 4.2 – Fuel System Design, March 2007.